Supporting Information

Synthesis of Silicon Nanoparticles from Rice Husk and their Use as Sustainable Fluorophores for White Light Emission

Sandeep Bose, Mohd. Azhardin Ganayee, Biswajit Mondal, Avijit Baidya, Sudhakar Chennu, Jyoti Sarita Mohanty, Thalappil Pradeep*

DST Unit of Nanoscience (DST UNS), and Thematic Unit of Excellence (TUE), Department of Chemistry, Indian Institute of Technology Madras, Chennai - 600 036, India

*Email: pradeep@iitm.ac.in

Index

Instrumentation

Si NPs were characterized by transmission electron microscopy (TEM), high resolution transmission electron microscopy (HRTEM), powder X-ray diffraction (PXRD), photoluminescence (PL), UV-Vis absorption and X-ray photoelectron spectroscopy (XPS). UV-Vis absorption spectra were measured using a Perkin Elmer Lambda 25 spectrophotometer in the range of 200-1100 nm. Photoluminescence measurements were performed using a Horiba JobinYvon Nanolog (FL 1000) fluorimeter. The band pass for excitation and emission was set at 3 nm. The excitation wavelength was set at 420 nm. Powder XRD was measured using Bruker D8 Advance diffractometer. The peaks at angles 28, 42 and 56 degrees correspond to (111), (220) and (311) planes of silicon nanoparticles. All the TEM/HRTEM and EDS measurements were done using JEOL 3010 (JEOL Japan) operating at 200 kV. SEM measurements were performed using FEI Quanta 200 operating at 30 kV equipped with EDS. XPS measurements were carried out using Omicron ESCA probe spectrometer with polychromatic Mg Kα X-rays ($h\upsilon$ = 1253.6 eV). The photostability studies were performed with a Philips TL 6W UV lamp. DLS measurements were carried out using Malvern Zetasizer Nano (ZSP) (Temperature, 25^{o}C; scan, 100; dispersant, water; refractive index, 1.33; viscocity, 0.08872 cP; dielectric constant, 78.5). A Jasco FT/IR-4100 type A spectrometer was utilized for recording the FTIR spectra (Scan, 64; resolution 4 cm^{-1}). All the

photographic images were taken with Nikon D5100 DSLR camera. Luminous flux measurements were carried out using Kusam Meco KM-Lux-99 digital Luxmeter.

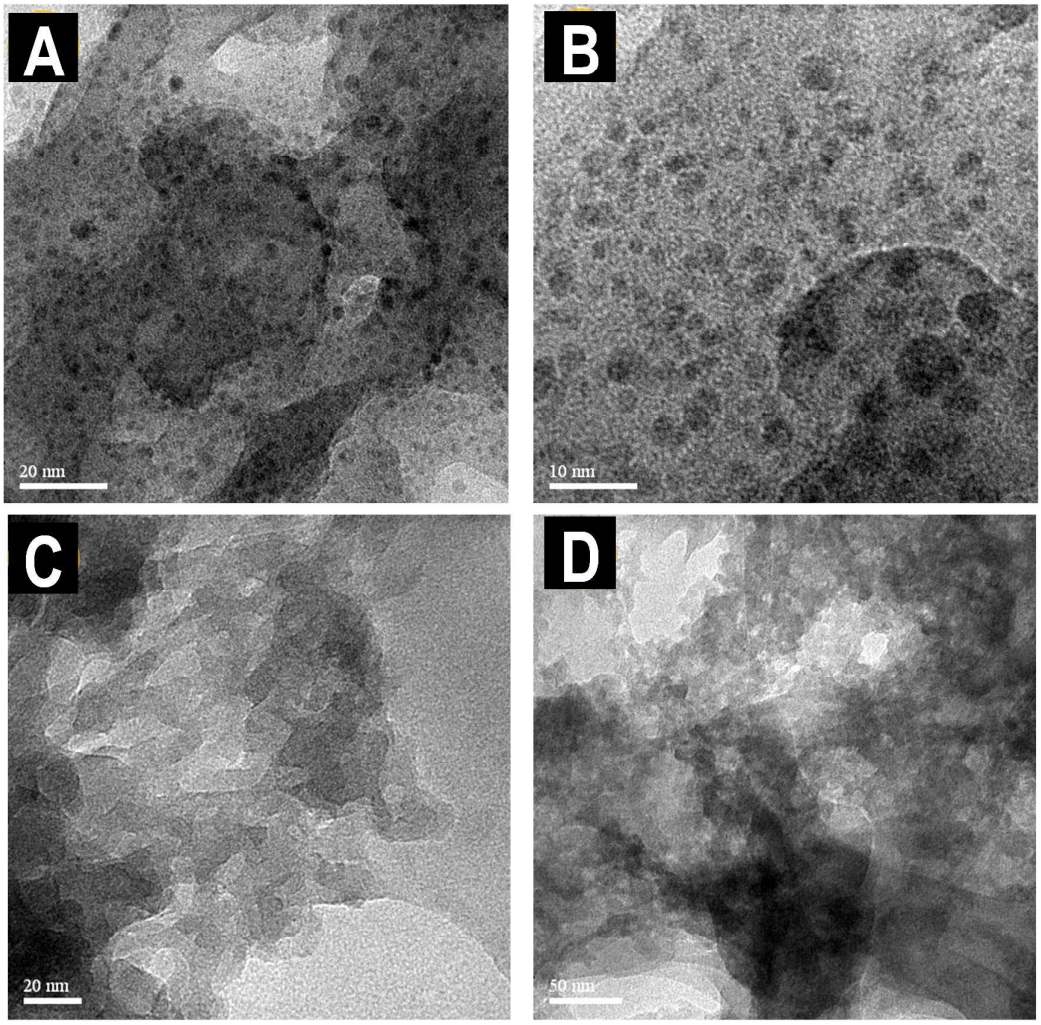

Figure S1. (A) & (B) TEM images of the SiNPs derived from the microwave treatment of rice husk powder & NaOH mixture. (C) & (D) TEM image of the rice husk powder and NaOH mixture showing the absence of nanoparticles without microwave treatment.

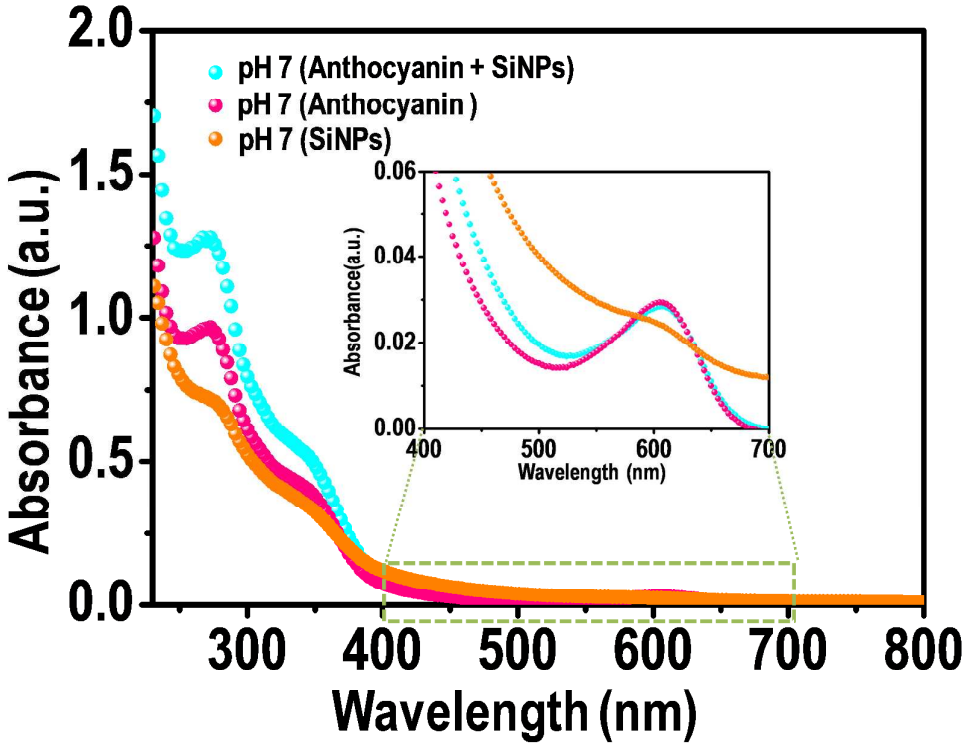

Figure S2. Absorption features of anthocyanin + SiNPs (cyan) at pH 7. Absorption features anthocyanin (pink) separated from Si NPs (orange) using molecular mass cut off centrifuge tubes shows absorption peak around 600 nm which is characteristic of anthocyanin and is absent in SiNPs.

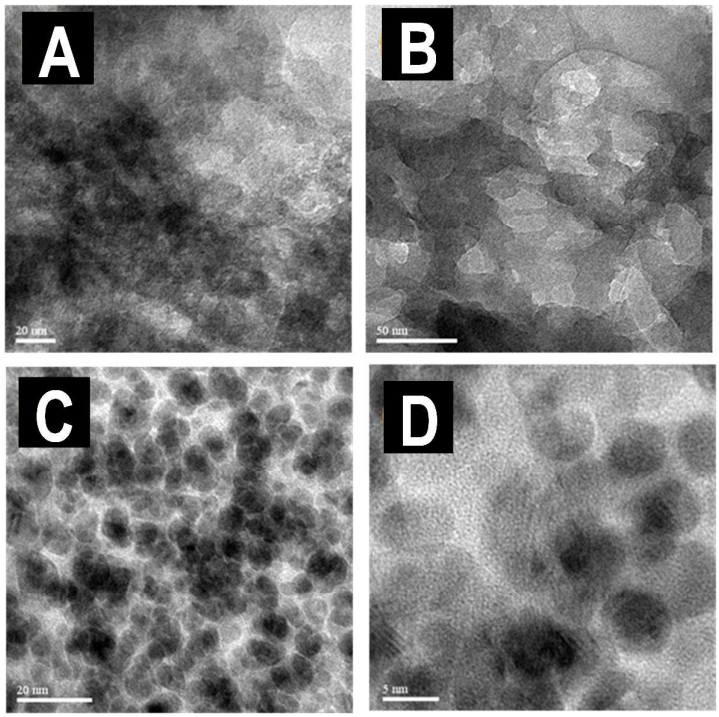

Figure S3. (A) & (B) shows the TEM image of the supernatant separated from the Si NPs using molecular mass cut off tubes which may contain silica and anthocyanin but no crystalline Si NPs. Similarly (C) & (D) shows the TEM images of the SiNPs separated. The Si NPs were collected as residue where as anthocyanin was collected as supernatant. This method of separation SiNPs from anthocyanin was quite efficient.

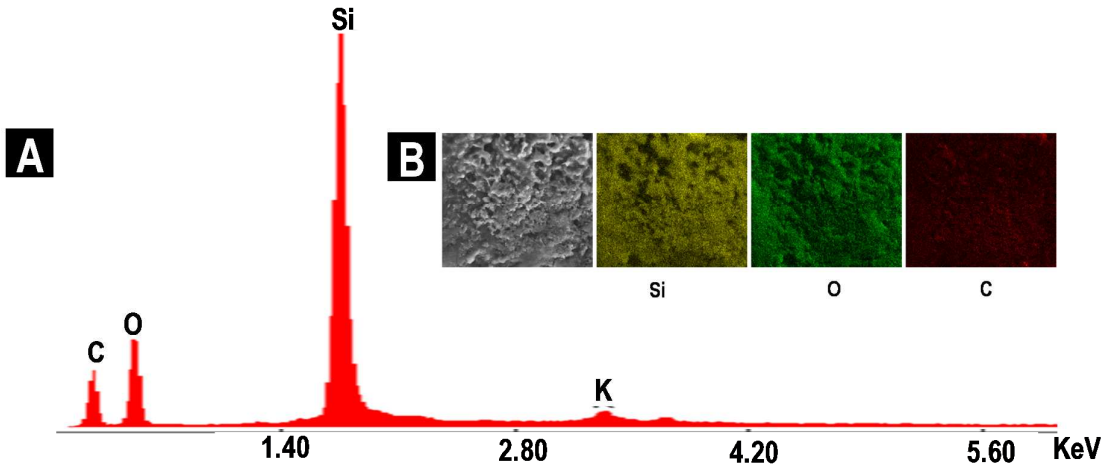

Figure S4. (A) SEM-EDAX spectrum of rice husk powder. (B) Elemental mapping of rice husk powder to show the elements present in it. It is clearly evident that rice husk contains high quantity of silicon in the form of silica. The carbon and oxygen are coming from the cellulose/hemicellulose and silica present in rice husk.

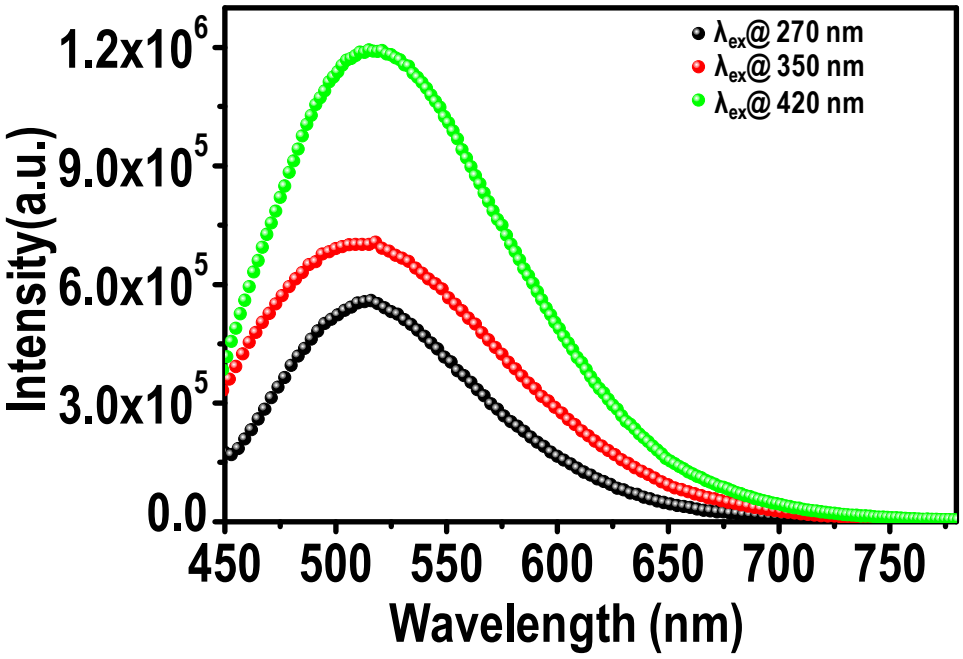

Figure S5. Excitation wavelength dependent emission spectra of Si NPs shows no shift in emission on changing the excitation wavelength.

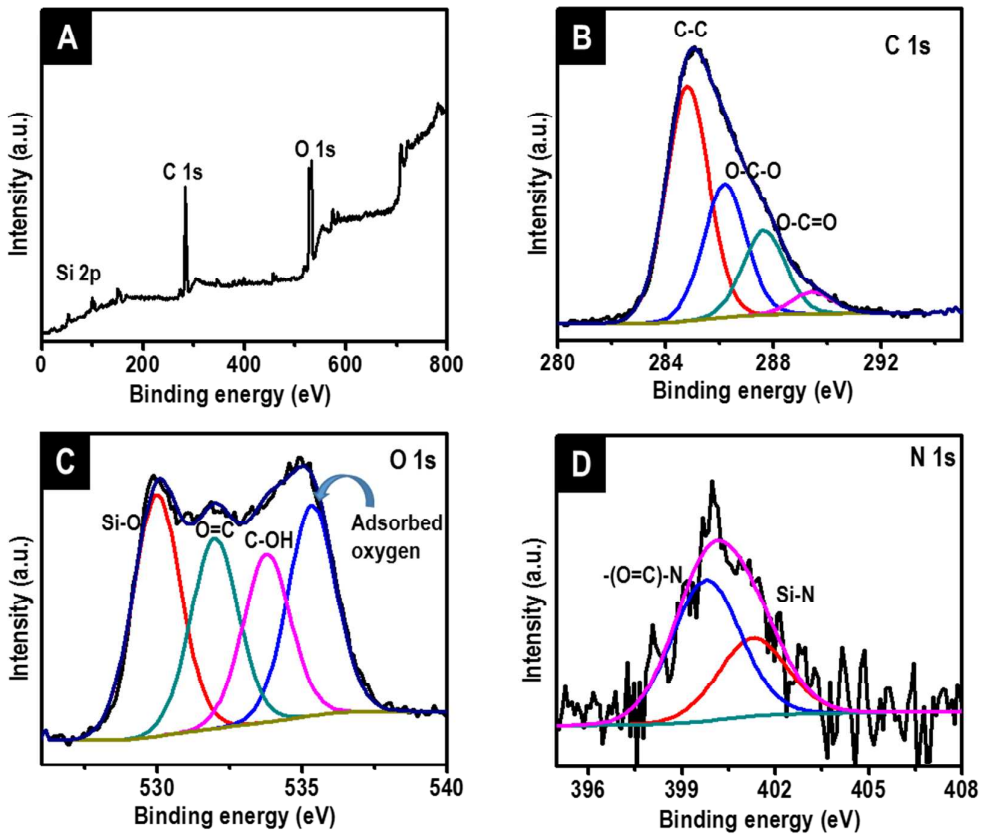

Figure S6. (A) Full range XPS spectrum of the Si NPs. (B), (C), (D) shows the C 1s, O 1s, N 1s spectra of microwave synthesized Si NPs respectively.

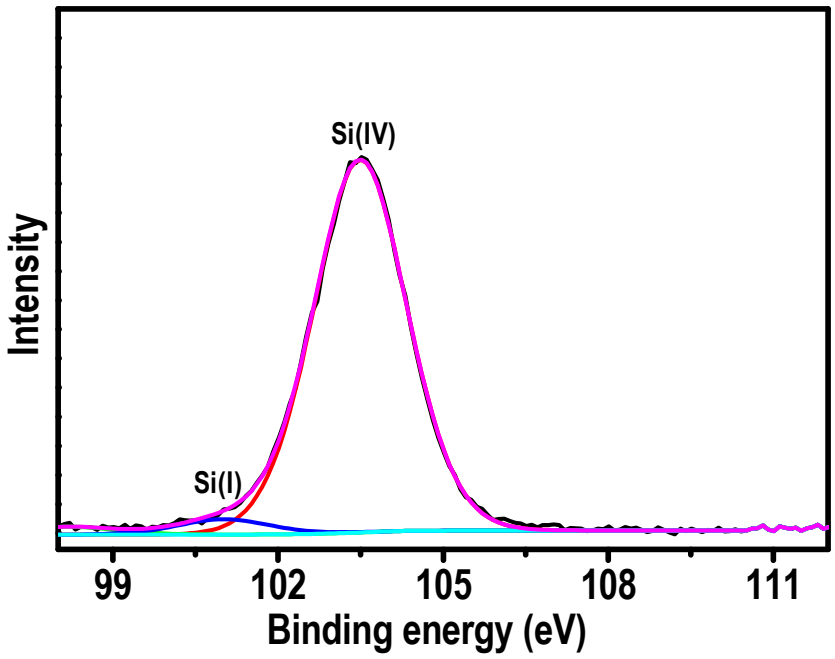

Figure S7. XPS spectrum of (rice husk powder + NaOH) mixture. It shows the absence of Si(0) features and only Si(IV) features are present. The Si(0) features at 99.6 eV appears only after microwave irradiation.

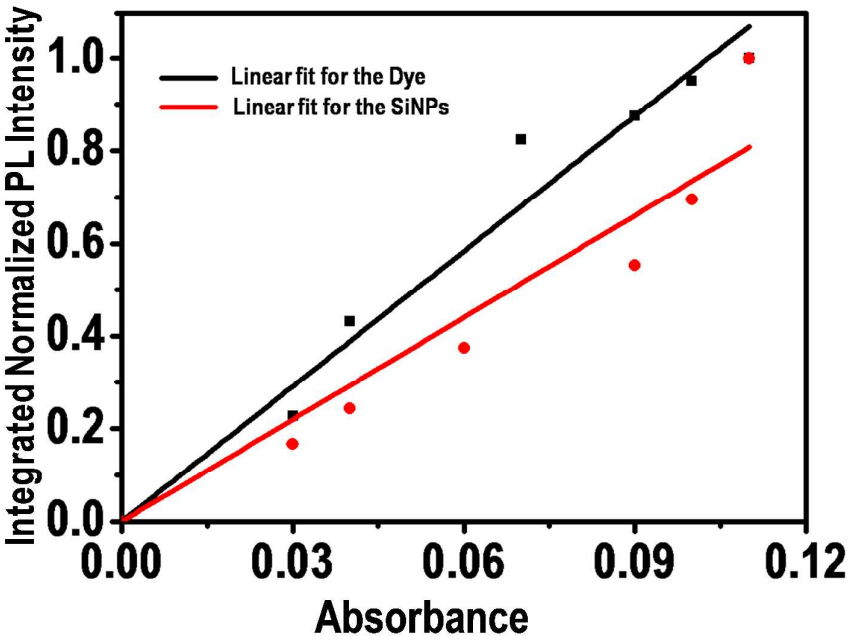

Figure S8. Plot of normalized PL intensity against absorbance to calculate slope (K) of the graph. The quantum yield was calculated to be 0.58.

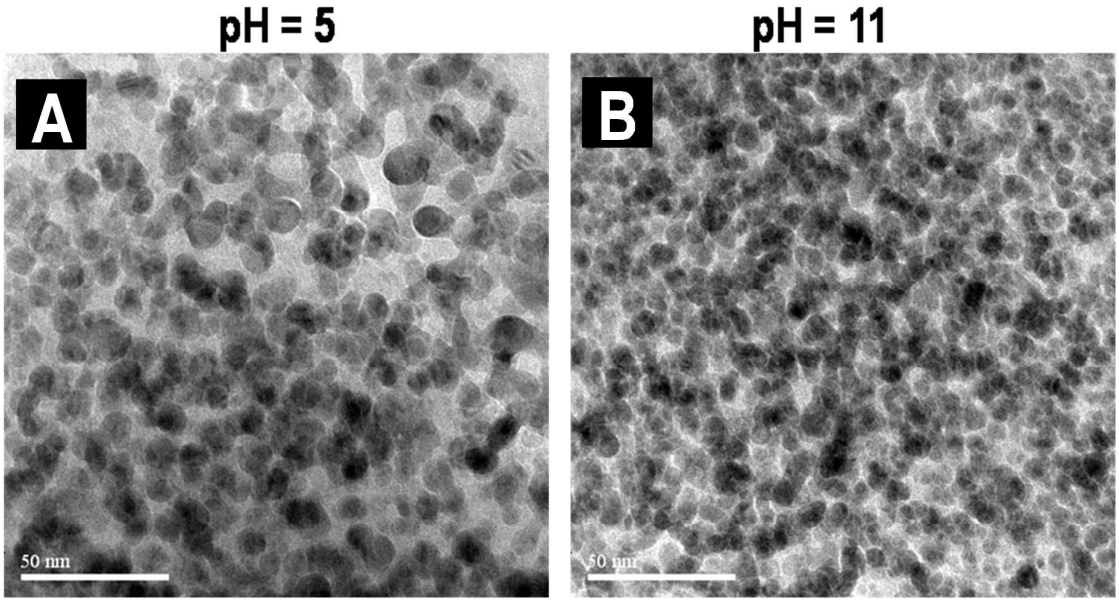

Figure S9. (A) & (B) are TEM images of Si NPs at pH 5 & 11 ensuring the existence of Si NPs i.e. the stability of nanopaticles do not change on changing pH.

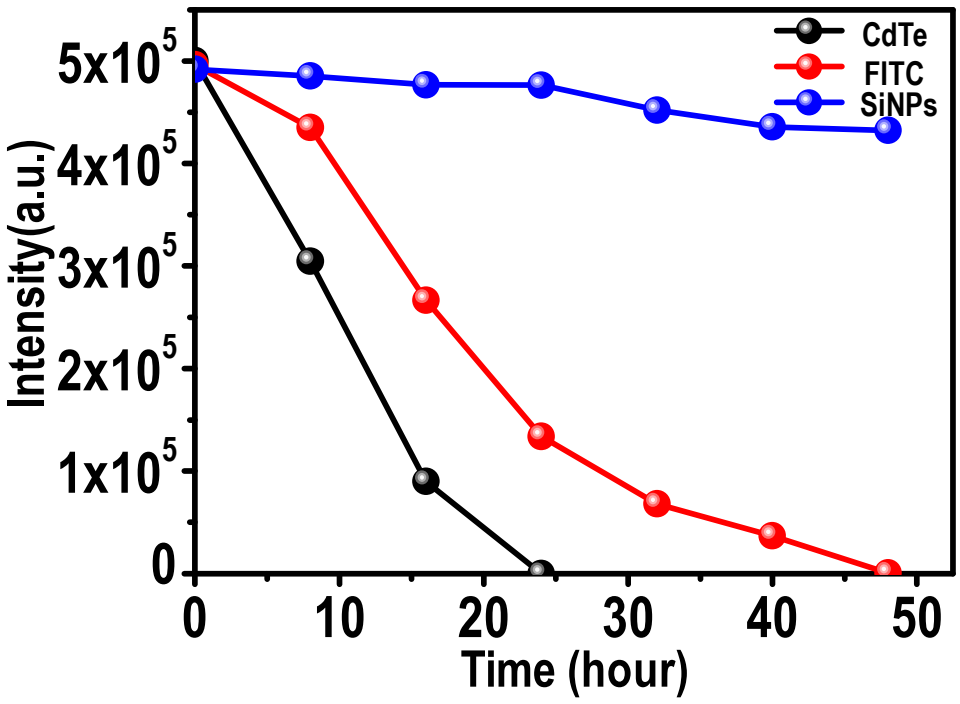

Figure S10. Plot of PL intensities of CdTe, FITC, Si NPs as a function of time.

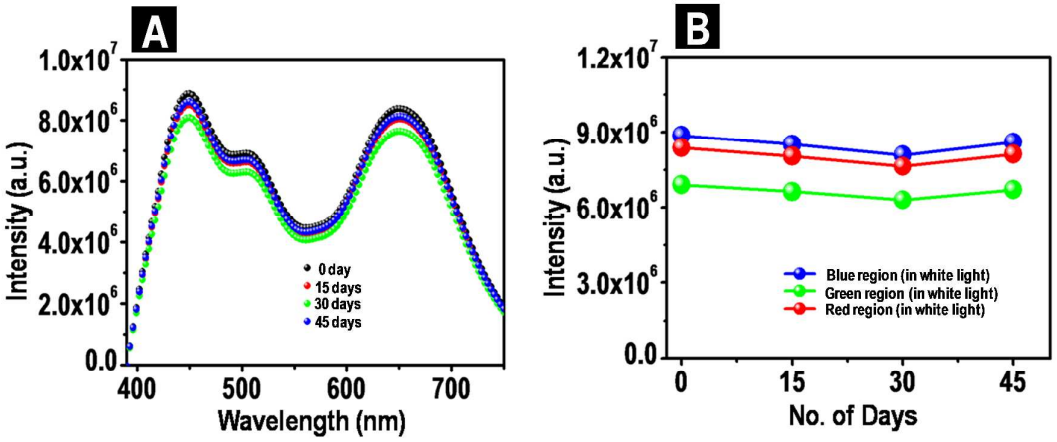

Figure S11. (A) Plot of the resulting white light emission of the mixture as a function of wavelength at different time interval to check the stability of material. As white light is a mixture of 3 colours i.e. blue, green & red, white light PL show three different regions namely blue emitting region, green emitting region, red emitting region. Figure (B) is a plot of intensity variations of different regions of white light over a period of 45 days.

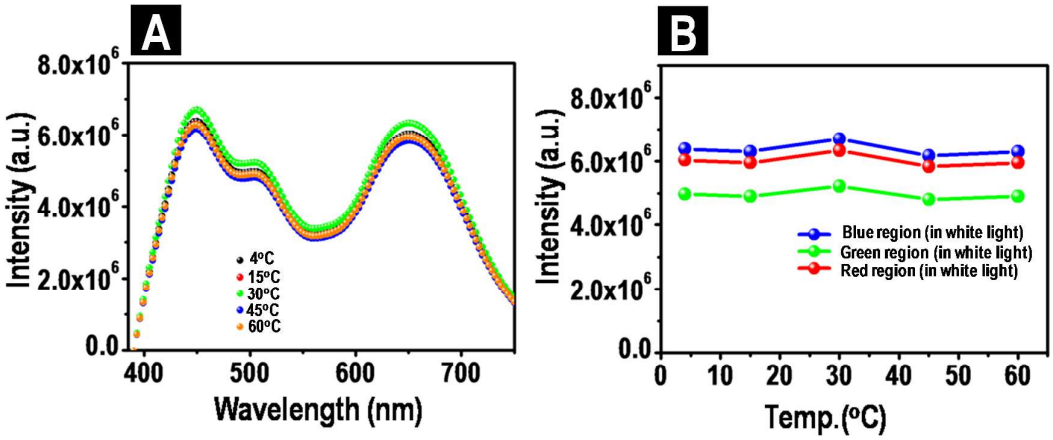

Figure S12. (A) Plot of resulting white emission of the material as a function of wavelength at different temperatures of the solution to check the thermal stability of the material. (B) Plot of PL intensities of different regions i.e. blue, green & red regions of white light as a function of temperature.Almost no change in intensities were observed indicating thermal stability of the material over the measured range of temperature.

Figure S13.(A) & (B) shows the excellent hydrophilic nature of the as-prepared Si NPs where organic solvents having different densities i.e. DCM and Hexane were used to check its miscibility with water dispersible Si NPs.

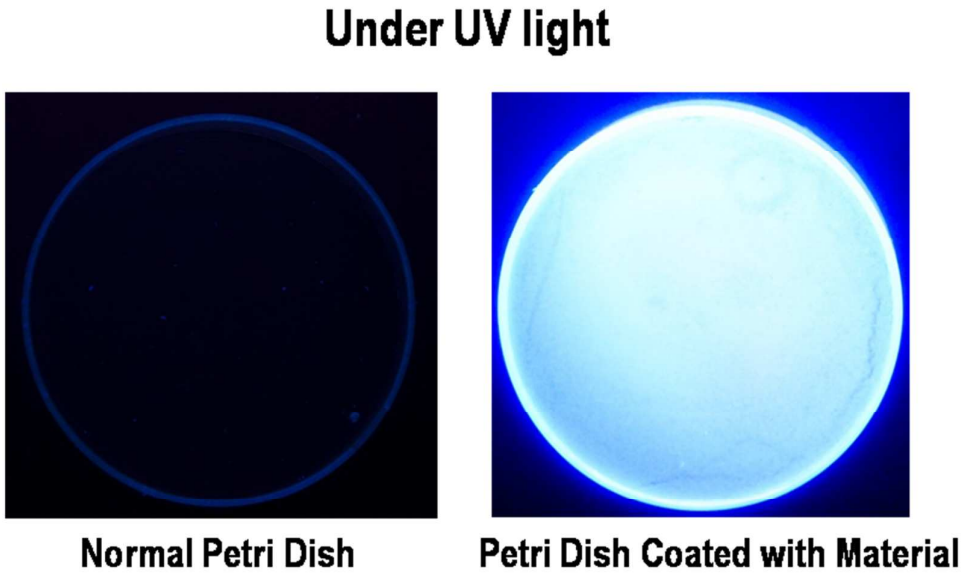

Figure S14. Photographic image of the normal perti dish and petri dish coated with material under UV light.

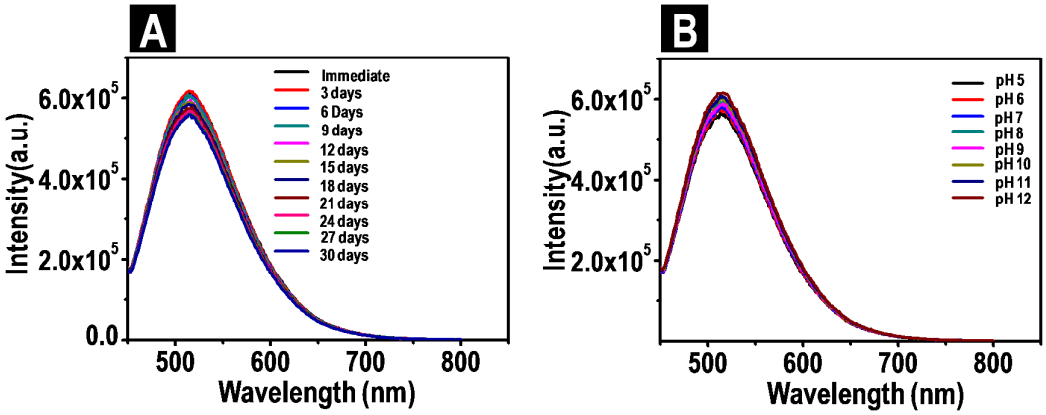

Figure S15. (A) Time dependent photoluminescence spectra of the green luminescent Si NPs. (B) pH dependent photoluminescence spectra of the Si NPs.